High Efficiency O-band Preamplified Receiver Integrated with Semiconductor Optical Amplifier and Uni-travelling Carrier Photodiode for Passive Optical Network

Risab Gnanamani, Hervé Bertin, Claire Besancon, Karim Mekhazni, Christophe Caillaud, Marina Deng, Mukherjee Chhandak, Cristell Maneux

High efficiency O-band SOA-UTC preamplified receiver for passive optical network (PON)

Risab Gnanamani, Hervé Bertin, Claire Besancon, Karim Mekhazni , Christophe Caillaud, Marina Deng, Chhandak Mukherjee, Cristell Maneux*

R. Gnanamani, H. Bertin, C. Besancon, K. Mekhazni, C. Caillaud

III-V Lab, A Joint Lab between Nokia Bell Labs, Thales Research & Technology and CEA-LETI, 91767 Palaiseau, France

E-mail: Risab.gnanamani@3-5lab.fr

R. Gnanamani, M. Deng, C. Mukherjee, C. Maneux

IMS Laboratory, University of Bordeaux, UMR CNRS 5218, 33405 Talence, France

Keywords - High speed photodiode, Semiconductor Optical Amplifier (SOA), Uni-Travelling Carrier Photodiode (UTC-PD), Photonic Integrated Circuit (PIC)

Abstract – With the continuous increase in data traffic and enormous consumption of data in terms of video on demand services and cloud computing, there is an increasing demand for high speed and high sensitivity short reach receivers for PON (Passive Optical Networks) access network which are point to multi-point networks. Avalanche photodiodes (APD) are the standard receivers in PON networks due to their high sensitivity and low cost. However, it is currently not clear if they can provide high bandwidth above 40 GHz with good performance (gain, noise, etc.). Furthermore, standard PIN photodiodes do not provide sufficient sensitivity for PON networks. Therefore, we propose in this article a SOA-UTC receiver which is a photonic integrated circuit (PIC) comprising a semiconductor optical amplifier (SOA) for optical preamplification and a high-speed uni-travelling-carrier (UTC) photodiode for opto-electronic conversion. We demonstrated a very high responsivity of 140 A/W, with a Polarization Dependent Loss (PDL) around 1 dB and a 3-dB bandwidth of 48 GHz, which is very promising for future PON network with 50 Gbit/s capacity and above.

1. Introduction

The rapid evolution of data consumption, driven by mobile communication, remote work, internet video services and cloud computing, has increased the demand for bandwidth exponentially. Consequently, the devices currently deployed in PON access networks need to be upgraded to meet these demands. However, APD receivers that are commonly used in

Passive Optical Network (PON) suffers from limited gain×bandwidth product which prevent them from providing simultaneously high bandwidth and high responsivity. For example, recent results on SiGe vertically illuminated APD shows a limited responsivity of 3.1 A/W for a moderately high bandwidth of 25 GHz.[1]

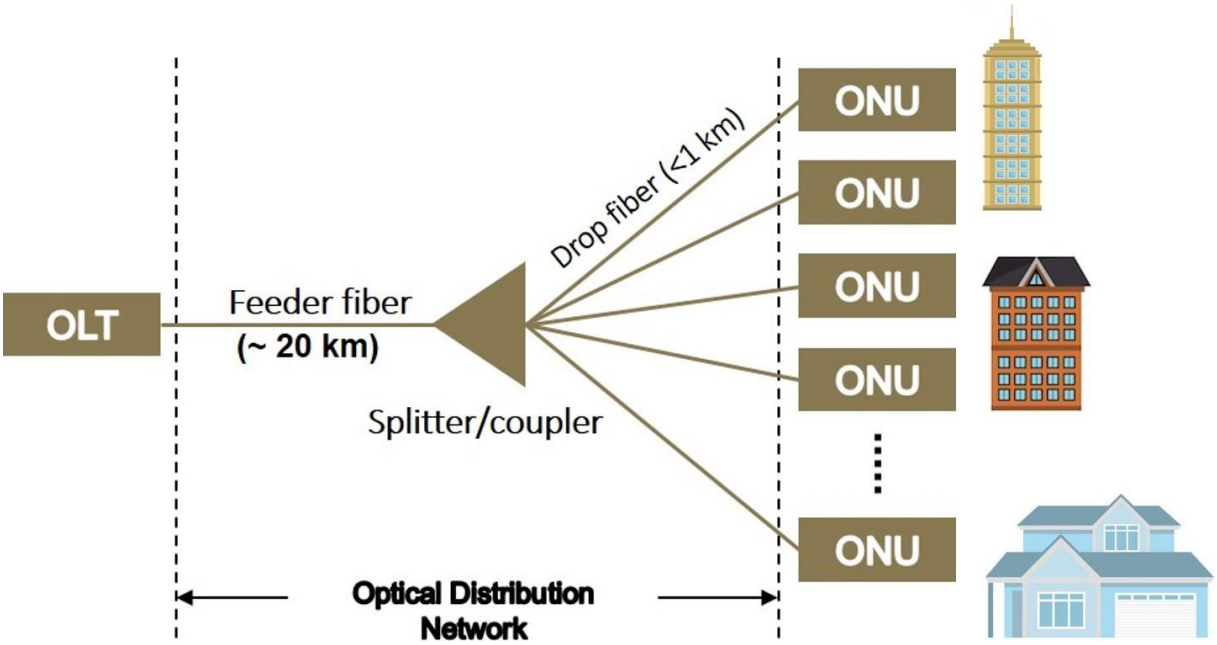

Figure 1. Schematic view of a PON access network

Figure 1 shows the schematic of the optical distribution network (ODN) of a typical PON access network. It is a point to multi-point network in which the Optical Line Terminal (OLT) on the operator side is typically connected to 32 to 64 Optical Network Unit (ONU) on the user side (Fiber to the home/FTTH customers, radio unit, and enterprise). Associated with a transmission distance up to 20 km, this result in a minimum optical budget of 29 dB for the network.[2]

50Gbit/s PON (50G-PON/HS-PON) has recently been normalized and will likely replace current G-PON (2.5 Gbit/s) and XGS-PON (10 Gbit/s) networks [2] and the upcoming topic for research is 100 to 200 Gbit/s PONs. These very high speed PONs will need to work with existing ODN which means that a very good receiver sensitivity will be required despite bit rate increase (-22.7 dBm minimum for 50G-PON in upstream according to ITU-T G9804.3).[3] **Figure 2** shows the existing state-of-the-art of high-speed photodiodes.[1][4-15] As APDs' performance decrease very fast with their bandwidth and become comparable to standard PIN above 50 GHz bandwidth, we propose to use pre-amplified receivers in to have simultaneously wide bandwidth and high sensitivity. We recently presented early results on an SOA-UTC

receiver with a record high responsivity of 140 A/W for future access network above 50 Gbaud.[16] In this article, we present extended characterizations and analysis of the SOA-UTC and demonstrated a 3-dB bandwidth above 70 GHz with the integration of a biasing circuit.

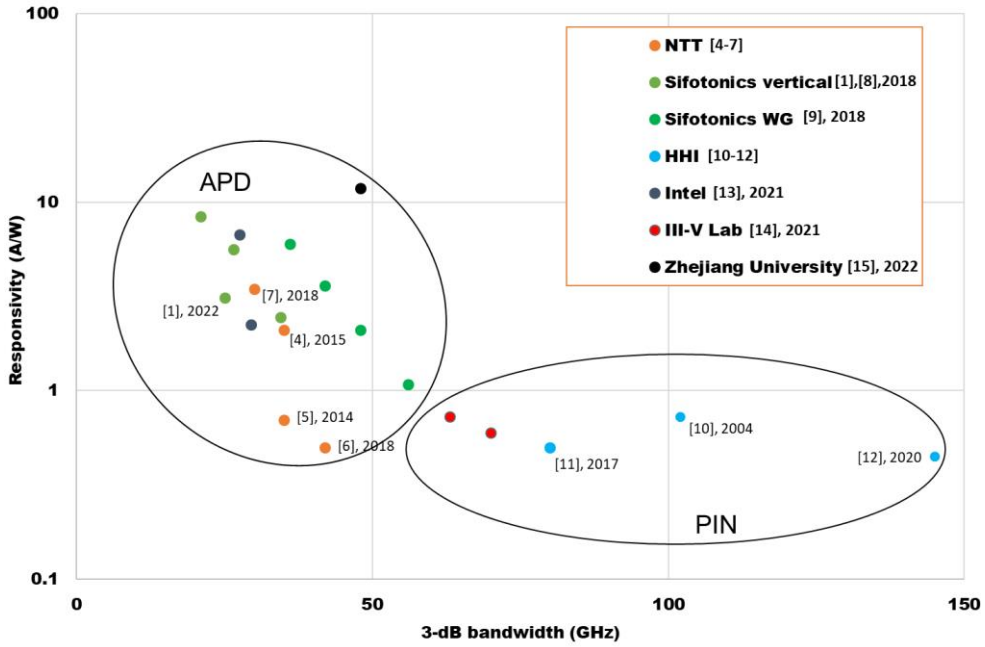

Figure 2 Current state-of-the-art of high-speed photodiode

Semiconductor Optical Amplifier (SOA)

SOA is an amplifier with active semiconductor medium that amplifies the incoming optical power. As shown in **Figure 3**, SOA is made of a PIN junction similar to that of a laser diode. The intrinsic region of the device acts as the active part of the device: under electrical injection, electrons move to the conduction band, which allow amplification of the incoming signal by the stimulated emission process. However, this induce also spontaneous emission (SE), which is then amplified by stimulated emission: this amplified spontaneous emission (ASE) create noises, which degrade the signal quality.

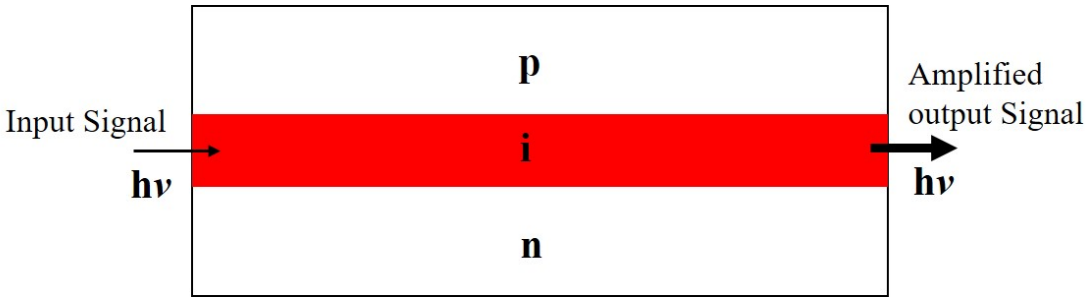

Figure 3 Principle of operation of a SOA

Uni-Travelling Carrier Photodiode (UTC-PD)

The UTC-PD is a pin-PD, in which only electrons are used as active carriers, thus greatly enhancing the performance of the device, especially achieving the high speed.[17]. As shown in **Figure 4**, the photodiode structure uses a p-doped absorber zone in which electrons and holes are generated. The latter are collected by the p-contact by dielectric compensation, which has a response time in the ps range for doped layers. Therefore, their contributions to the transit time is negligible. The electrons diffuse towards the depleted area, called the collector, where they are accelerated under the effect of the electric field and drift towards the n-contact area.

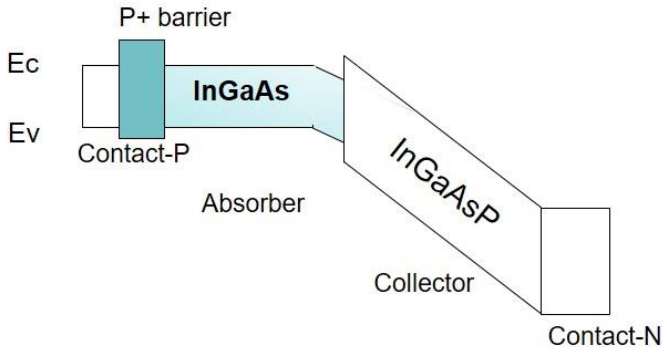

Figure 4 Band structure of the UTC-PD

2. Device description and technology

Our device monolithically integrates a SOA and a uni-travelling carrier photodiode (UTC-PD) and is shown in **Figure 5.a**. The SOA is a buried heterostructure and the photodiode is made with deep ridge structure on a semi-insulating InP substrate.[18] The SOA has an active waveguide made of a tensile strained InGaAsP to obtain a low TE/TM polarization dependent loss.[19] A passive waveguide with buried and planar section connects the SOA and the photodiode. As schematically shown in **Figure 5.b**, the light from the fibre first enters into the fibre waveguide, which is a waveguide with a large mode area (around 4-µm mode diameter) to allow low coupling losses with a lensed fibre. From there, the light is coupled into the active waveguide adiabatically, in which it is amplified. Then the light is coupled to the buried section of the passive waveguide, which then transforms into a planar section where the light is evanescently coupled with the photodiode.[18] In the previous designs of III-V Lab, the optical mode had to descend to the fibre waveguide before reaching the passive waveguide to reduce the risk of backward reflection at the Butt Joint (BJ) interface between the SOA waveguide and the passive waveguide.[18] The new design allows us to localize current injection only in straight waveguide and not in tapered section, resulting in higher energy efficiency, lower component

footprint and a better responsivity. The SOA, the passive waveguide and the photodiode sections were grown with Metal Organic Vapour Phase Epitaxy (MOVPE). The SOA waveguide and parts of the passive waveguide were also buried using MOVPE, with p-type InP and InGaAs for contact layers. The active and passive waveguides were defined using e-beam lithography and etched using RIE plasma etching. The photodiode comprises of a InGaAsP collector with 300nm thickness and a 200nm gradient-doped InGaAs absorber. The gradient doping within the absorber was implemented to generate an electric field to accelerate the electrons.[17] The photodiode mesa was defined using a mix of Inductively Coupled Plasma (ICP) dry etching and wet etching, and the passivation was done using ICP-SiN_x deposition. The SOA-UTC chips were then cleaved and an Anti-Reflection (AR) coating was deposited on their input facet.

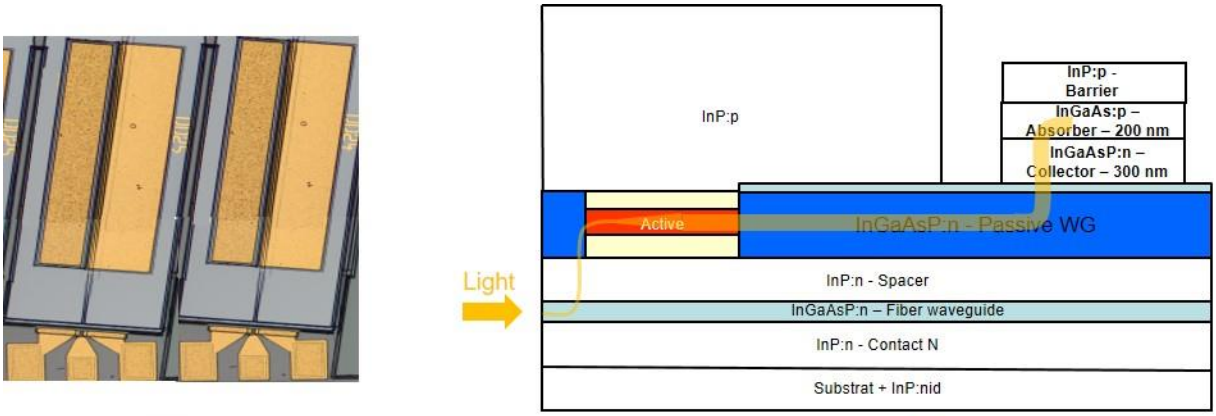

Figure 5. a) Optical microscope image of 2 SOA-UTCs. **b)** Schematic view of the structure

3. Device Characterizations

Measurements were performed with a lensed fibre with mode diameter of 4.4 µm, at a temperature of 20°C. The amplified spontaneous emission (ASE) spectrum of the SOA-UTC with of a 500µm long SOA is measured using an optical spectrum analyser (OSA) with a resolution of 10 picometer for various SOA drive currents, as shown in **Figure 6**. The peak wavelength varies from 1360 nm at 20 mA to 1323 nm at 100 mA. We obtain a broad 3-dB optical bandwidth of above 60nm at 100 mA SOA drive current, with negligible ripples below 0.5 dB, showing that parasitic internal reflection inside the device is also negligible. The dip in the ASE spectrum at long wavelengths (>1330 nm) are exactly at the same wavelength for various devices and measurement conditions and are due to the OH absorption in the measurement setup (optical fibre and optical spectrum analyser). They do not impact our measurements performed at lower wavelengths. In addition to the SOA-UTCs, we also

characterized stand-alone UTC photodiodes on the same wafer featuring multiple dimensions. **Figure 7** shows the dark currents we obtained from the stand-alone photodiodes and photodiodes integrated with the SOA. Typical values for the given dimensions range between 1-30 nA for a bias range of 0 to -2V. These very low dark current values indicates a very good quality of the mesa passivation and the optimisation of the junction of the photodiode. This will also ensure a high signal to noise ratio (SNR).

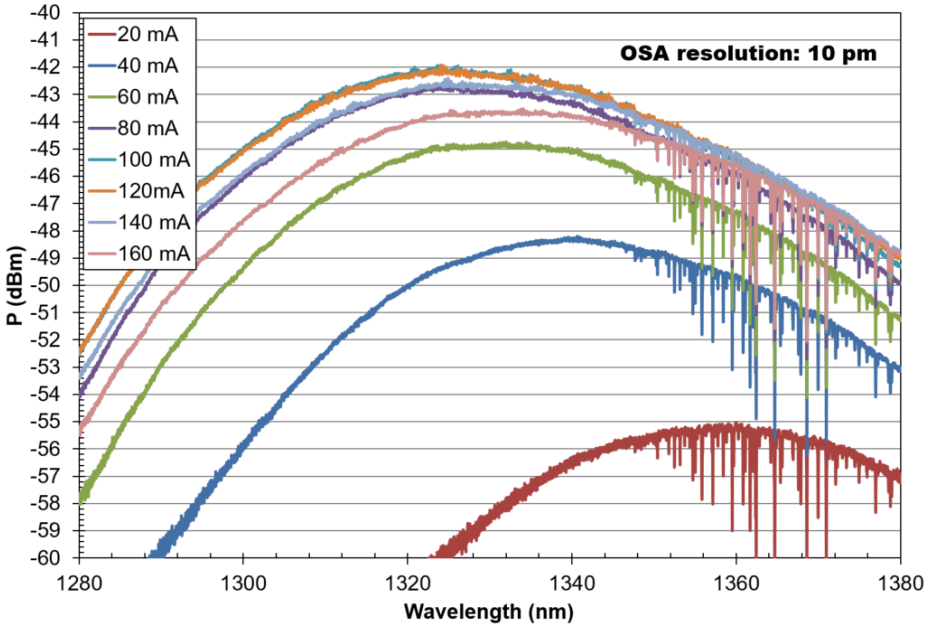

Figure 6. ASE spectrum of a SOA-UTC at various SOA currents

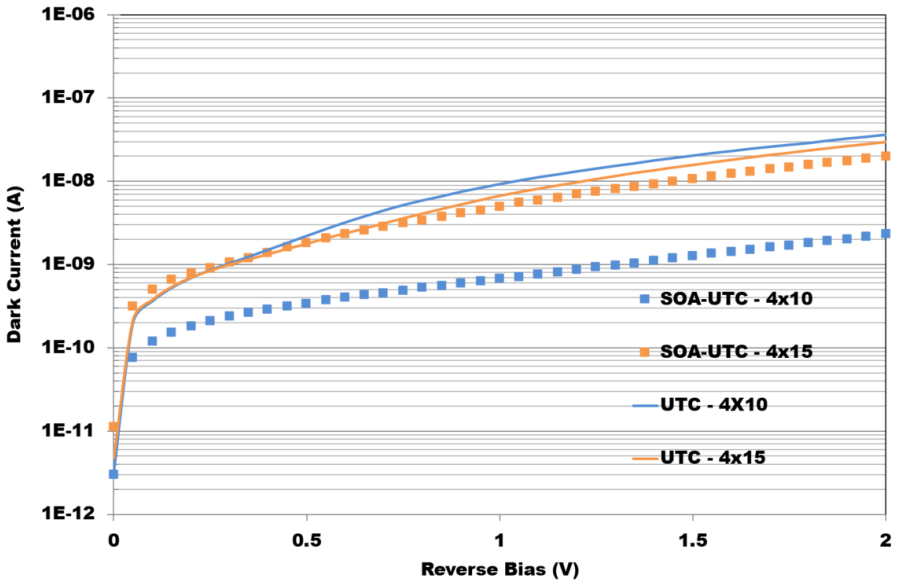

Figure 7. Dark current measurements of Stand-alone UTCs and SOA-UTCs

We also measured the responsivities of our devices at different SOA currents for various wavelengths in the O-band. Using a SOA-UTC with a 500 µm long SOA and a 4×15 µm²

photodiode, at 1310 nm, we reached a record responsivity close to 140 A/W at a 140 mA SOA drive current and still ensuring a responsivity of 80 A/W at a 80 mA drive current **(Figure 8.a)**, which showcases nearly 50 % improvement compared to our previous demonstration (90 A/W at 160 mA drive current).[18]

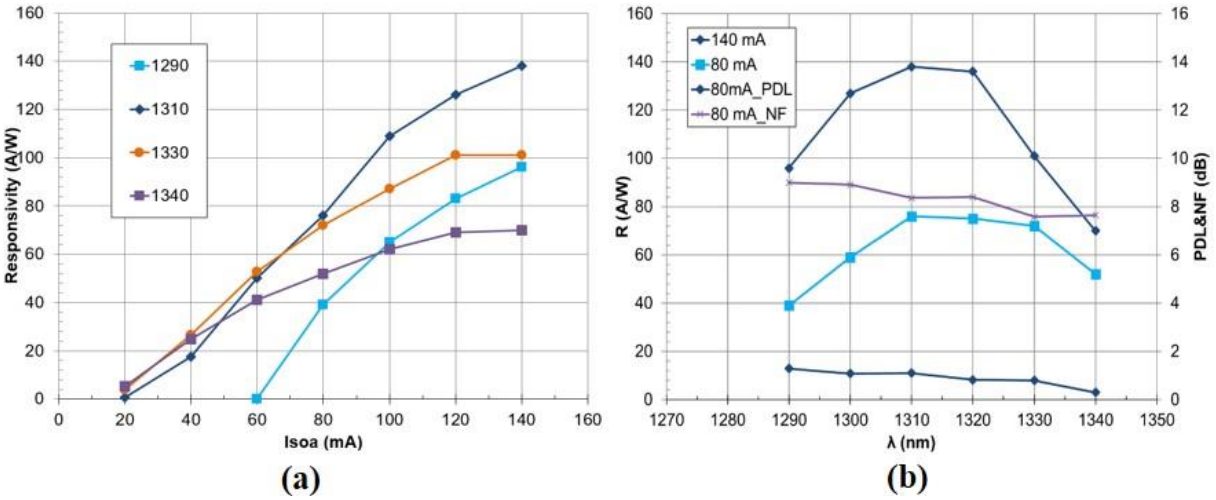

Figure 8. a) Responsivity, **b)** Gain, PDL and NF of a SOA-UTC (500µm long, 4x15µm^2 PD), at various wavelengths

Figure 8.b presents the PDL (polarisation dependent loss) and NF (noise figure) values that we have calculated from the measurements. PDL is calculated with Equation 1, with the measured minimum (R_{min}) and maximum responsivity (R_{max}) values with respect to change in polarization. While operating at the right side of the gain peak, we obtain a very low polarisation dependent loss of around 1 dB.

$$PDL_{dB} = 10 \times \log_{10}(R_{min}/R_{max}) \quad (1)$$

Noise figure of the SOA is measured directly on the integrated component because we don't have test SOAs and to have measurement on the final device. For this calculation, we use the formulas and hypothesis described below. By assuming homogeneous ASE over the bandwidth resolution Bo of the OSA (10 pm, converted in Hz), the ASE power emitted in one mode is,

$$P_{ASE}(v) = n_{sp} h v (G-1) B_o \quad (2)$$

Where n_{sp} the spontaneous emission factor, h the planck's constant, v the frequency, and G the single mode pass gain. For a polarization independent amplifier, the spontaneous emission of the TE and TM modes are similar. Considering η_{abs} the part of the light coming out of the SOA which is absorbed in the photodiode, the current generated by the ASE in the photodiode for a high gain (G>>1) can be expressed as,

$$I_{ASE}(v) \approx 2 \frac{q}{hv} n_{sp} h v G B_o \eta_{abs} \quad (3)$$

Considering η_e the coupling efficiency between the SOA and the input optical fibre,

$$I_{ASE}(v)\,\eta_e = 2\,\frac{q}{h\nu}\,n_{sp}h\nu G B_o \eta_{abs}\eta_e = 2n_{sp}h\nu B_o R \quad (4)$$

In Equation 4, R is the responsivity. The NF can be expressed as,

$$NF = \frac{2n_{sp}}{\eta_e} = \frac{I_{ASE}(v)}{h\nu B_o \mathrm{R}} \quad (5)$$

However, Equation 5 should be corrected for polarization dependent SOA. [20]

$$NF = \frac{2n_{sp}}{\eta_e} = \frac{I_{ASE}(v)}{h\nu B_o R_{max}} \times \frac{2}{1 + R_{min}/R_{max}} \quad (6)$$

To obtain $I_{ASE}(\upsilon)$, we integrate the ASE spectrum to find the portion of the power at the wavelength (at the corresponding frequency υ) and assume constant absorption in the photodiode to allow the calculation. With Equation 6 and associated hypothesis, we obtain a noise figure (NF) between 8.9 dB to 7.6 dB in the 1290-1340nm range **(Figure 8.b).** The obtained NF is comparable with previous results of SOA-UTC devices using the same method (8 dB at 1270 nm and 6.6 dB at 1310 nm for an internal SOA gain of 22.9 dB[18], and ~8 dB of NF in C-band, with an internal SOA gain of ~20 dB.[21] To estimate the coupling losses, we reverse biased the SOA so that it acts as a photodiode and measured 75% quantum efficiency. As the SOA is very long, we can assume 100% of absorption of the light coupled into the SOA active waveguide. Therefore, the coupling losses (fibre to fibre waveguide, and taper to couple the light into the active SOA waveguide) are around 25% (1.25 dB).

As shown in **Figure 9.a**, using a 400 µm long SOA, we have a peak responsivity above 40 A/W at 1310 nm, a low PDL below 1 dB (<0.5 dB at 1340 nm) and a lower noise figure, down to 6.8 dB. The reduction of the noise figure compared to 500 µm SOA can be attributed to a decrease of spatial hole burning inside the SOA, resulting in a better population inversion at the input and output of the SOA (Noise figure is mainly impacted by the input of the device).[22][23]

In **Figure 9.b**, we also compare the responsivities that we obtained from stand-alone photodiodes, which are nearly constant between 1280 nm and 1340 nm (very slight improvement when increasing the wavelength), with 0.41 A/W as maximum responsivity for a photodiode of dimension 4x15 µm^2. By comparing the maximum responsivities of the SOA-UTCs (140 A/W at 140 mA) and the stand-alone UTCs (0.41 A/W) for a 4×15 µm² photodiode at 1310nm, corresponding to 21.5 dB and -3.8 dB respectively, gives us the internal SOA gain of 25.3 dB for a 500 µm length. For SOA-UTCs with a 400 µm long SOA, we calculate an

internal gain of 19.9 dB, in agreement with the previous result (around 5 dB/100µm gain, assuming a linear operation of the SOA). The maximum responsivity that could be achieved by the photodiode is affected by the coupling loss at the input of the SOA (≤ 25%), the external quantum efficiency and the absorption coefficient of the photodiode.

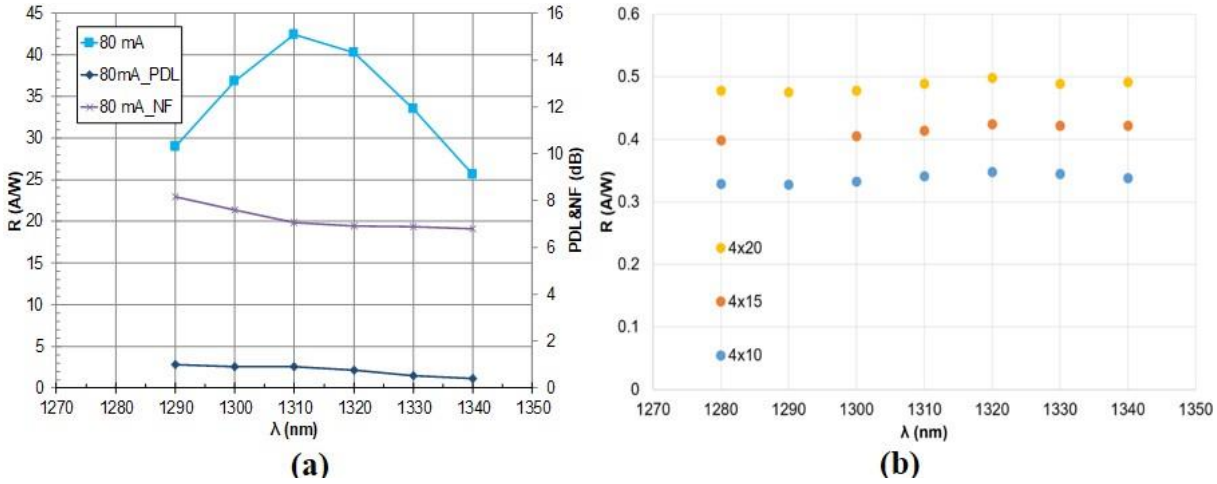

Figure 9. a) Gain, PDL and NF of SOA-UTC (500µm long, 4x15µm^2 PD), **b)** Responsivity of Stand-alone UTCs, at various wavelengths

We have also measured the S parameters of our devices, from which we have extracted the high frequency parameters such as junction capacitance (C_j) and series resistance (R_s) using the Open-Short method.[24] **Figure 10.a** and **Figure 10.b** shows the measured values of C_j and R_s respectively, and compares the UTC and SOA-UTC components of same dimensions. We could see that both values, especially C_j is quite flat across all frequencies. The extracted R and C values are thus quite promising to obtain an increased bandwidth of the device. In addition, we can see that the values of each dimension between UTC and SOA-UTC components are almost similar, which ensures a good process credibility.

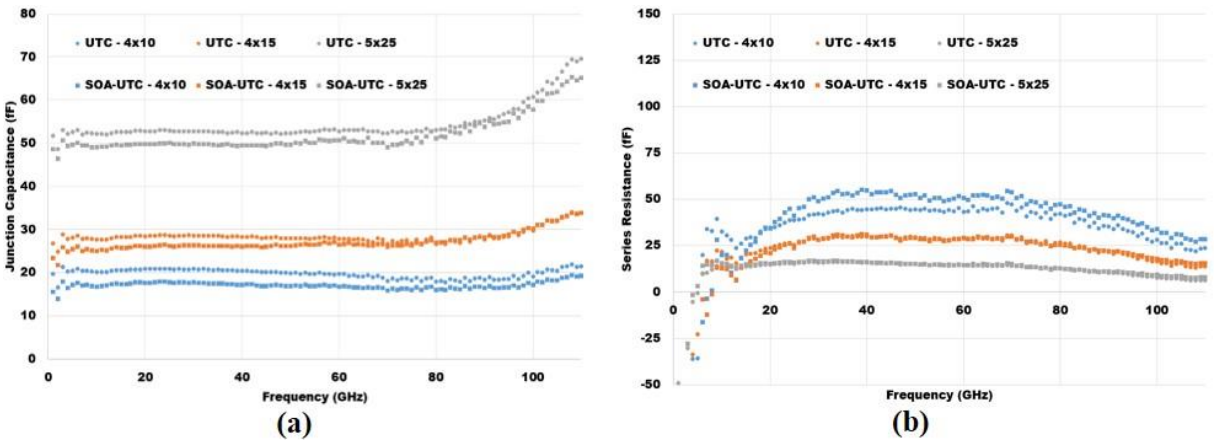

Figure 10. a) Junction capacitance and **b)** Series resistance of UTC and SOA-UTC of different dimensions

We have also implemented some diodes with an integrated biasing circuit as shown in **Figure 11**. The biasing circuit comprises of a decoupling capacitor and 50 Ohm matching resistor, resulting in an effective 25 Ohm load for the photodiode when connected to 50 Ohm high frequency devices like power meter.

We measure the frequency response of our devices at different bias voltages and photocurrents, and in **Figure 12** we show the curves at -1V bias and 1 mA of photocurrent. The highest 3-dB bandwidth we have obtained for devices without biasing circuit is 49 GHz with the 4x10-μm^2 SOA-UTC. It starts to decrease with increasing photodiode dimensions due to increase in photodiode capacitance and therefore lower RC cut-off frequency.

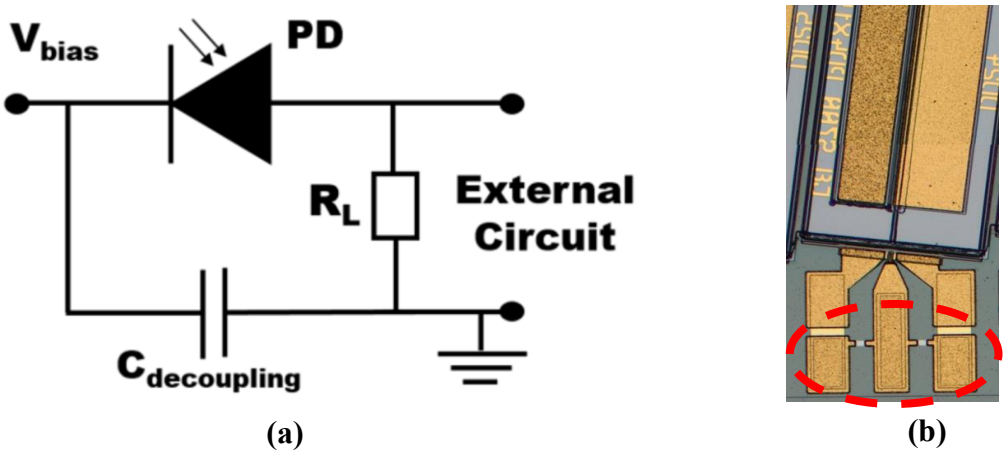

Figure 11. a) Schematic diagram of a photodiode with biasing circuit **b)** Optical microscope image of a SOA-UTC with biasing circuit highlighted in red circle

With the help of the biasing circuit, the bandwidth is significantly improved. As can be seen in **Figure 12**, the integration of biasing circuit helped to achieve a bandwidth more than 70 GHz, for a 5x25-μm^2 diode instead of 40 GHz without the biasing circuit. In the same fashion, we expect the smaller diodes such as 4x10 μm^2 and 4x15 μm^2 to reach the 3-dB bandwidth above 100 GHz. On the contrary, we have obtained the highest bandwidth of only 42 GHz for a stand-alone PDs. This difference in bandwidth between the SOA-UTCs and stand-alone UTCs is reproducible across different wafers that followed same process technology, but there is not yet a definitive conclusion for this behaviour.

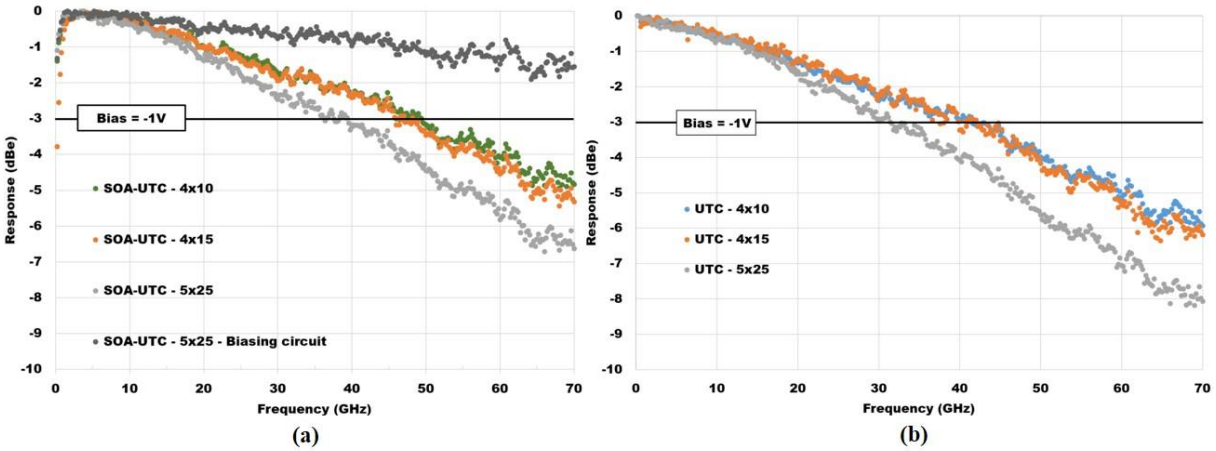

Figure 12. Frequency response of **a)** SOA-UTC and **b)** UTC of different dimensions

On the other hand, the similar or nearly similar bandwidth of smaller dimension diodes (4x10-μm^2 and 4x15-μm^2) means that the smaller diodes are transit time limited. In addition, these bandwidths are lower than the bandwidth of 70 GHz measured for stand-alone UTCs in C-band that we have previously reported [14], even though their designs are similar (except a 400 nm collector in stand-alone UTC compared to 300 nm in SOA-UTC, which should have improved the transit time of SOA-UTC compared to previous stand-alone UTC) and also use a comparable process.[14] This could be explained by the higher doping level in the absorber contrary to what we have targeted **(Figure 13)**, which in turn induces dopant diffusion at the absorber collector interface. Therefore, electrons are slow down at this interface as they are not assisted by the electric field to pass through the potential barrier of the InGaAs/InGaAsP interface. This can be easily solved in a next fabrication to deliver high bandwidth/high efficiency SOA-UTC receiver. However, with the currently reported bandwidth, these devices are perfectly suitable for 50-100 Gbaud operation.

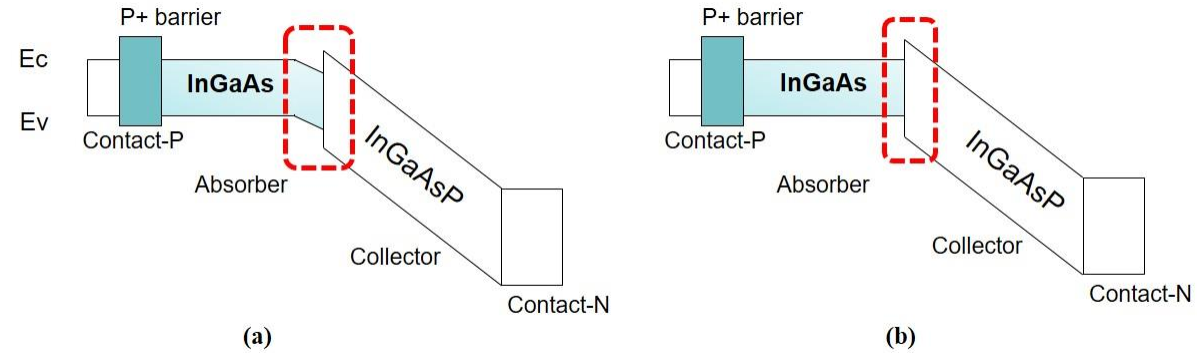

Figure 13. a) Targeted band structure vs **b)** Obtained band structure

4. Conclusion

In this work, we have developed a high efficiency pre-amplification receiver for PON access networks. We have presented SOA-UTCs and stand-alone UTCs for O-band applications with

record high responsivity of 140 A/W at a 140 mA SOA drive current, very low PDL of less than 1 dB and a noise figure between 8.9 dB to 7.6 dB. The SOA-UTCs are also shown to be more energy efficient owing to the passive taper. The bandwidth of the presented devices are suitable for practical operation in 50-100 Gbaud network. These performances can be further improved by solving the dopant diffusion issue we had in this fabrication run.

References

[1] C. Hong et al., "High Speed Ge/Si Avalanche Photodiode with High Sensitivity for 50Gbit/s and 100Gbit/s Optical Access Systems," 2022 Optical Fibre Communications Conference and Exhibition (OFC), San Diego, CA, USA, 2022, pp. 1-3.

[2] International Telecommunication Union, "ITU-G.9804.1: Higher Speed Passive Optical Networks - Requirements", https://www.itu.int/rec/T-REC-G.9804.1-201911-I/en, 11/2019

[3] International Telecommunication Union, “ITU- G.9804.3: 50-Gigabit-capable passive optical networks (50G-PON): Physical media dependent (PMD) layer specification“, https://www.itu.int/rec/T-REC-G.9804.3-202109-I/en, 09/2021

[4] M. Nada,H.Yokoyama,Y. Muramoto,T. Ishibashi, and H. Matsuzaki, “50-Gbit/s vertical illumination avalanche photodiode for 400-Gbit/s Ethernet systems,” Opt. Express, vol. 22, pp. 14 681–14 687, 2014.

[5] M. Nada, Y. Muramoto, H. Yokoyama, T. Ishibashi and H. Matsuzaki, "Vertical illumination InAlAs avalanche photodiode for 50-Gbit/s applications," 26th International Conference on Indium Phosphide and Related Materials (IPRM), Montpellier, France, 2014, pp. 1-2, doi: 10.1109/ICIPRM.2014.6880573.

[6] M. Nada, T. Yoshimatsu, Y. Muramoto, T. Ohno, F. Nakajima and H. Matsuzaki, "106-Gbit/s PAM4 40-km Transmission Using an Avalanche Photodiode With 42-GHz Bandwidth," 2018 Optical Fiber Communications Conference and Exposition (OFC), San Diego, CA, USA, 2018, pp. 1-3.

[7] M. Nada, Y. Yamada and H. Matsuzaki, "Responsivity-Bandwidth Limit of Avalanche Photodiodes: Toward Future Ethernet Systems," in IEEE Journal of Selected Topics in Quantum Electronics, vol. 24, no. 2, pp. 1-11, March-April 2018, Art no. 3800811, doi: 10.1109/JSTQE.2017.2754361.

[8] M. Huang *et al*., "Germanium on Silicon Avalanche Photodiode," in *IEEE Journal of Selected Topics in Quantum Electronics*, vol. 24, no. 2, pp. 1-11, March-April 2018, Art no. 3800911, doi: 10.1109/JSTQE.2017.2749958

[9] M. Huang et al., "56GHz Waveguide Ge/Si Avalanche Photodiode," 2018 Optical Fiber Communications Conference and Exposition (OFC), San Diego, CA, USA, 2018, pp. 1-3

[10] H.-G. Bach, A. Beling, G. G. Mekonnen, R. Kunkel, D. Schmidt, W. Ebert, A. Seeger, M. Stollberg, andW. Schlaak, "InP-based waveguide-integrated photodetector with 100 GHz bandwidth," IEEE J. Sel. Topics Quantum Electron., vol. 10, no. 4, pp. 668–672, Jul./Aug. 2004

[11] G. Zhou *et al*., "High-Power InP-Based Waveguide Integrated Modified Uni-Traveling-Carrier Photodiodes," in *Journal of Lightwave Technology*, vol. 35, no. 4, pp. 717-721, 15 Feb.15, 2017, doi: 10.1109/JLT.2016.2591266

[12] P. Runge, F. Ganzer, J. Gläsel, S. Wünsch, S. Mutschall and M. Schell, "Broadband 145GHz Photodetector Module Targeting 200GBaud Applications," 2020 Optical Fiber Communications Conference and Exhibition (OFC), San Diego, CA, USA, 2020, pp. 1-3

[13] M. Huang, K. Magruder, Y. Malinge, P. Fakhimi, H. Liao, D. Kohen, G. Lovell, W. Qian, K. Lee, C. Brandt, M. Hakami, Y. Chen, E. Carabajal, E. Guillermo, S. Slavin, and A. Liu, "Recess-type waveguide integrated germanium on silicon avalanche photodiode," in *Optical Fiber Communication Conference (OFC) 2021*, P. Dong, J. Kani, C. Xie, R. Casellas, C. Cole, and M. Li, eds., OSA Technical Digest (Optica Publishing Group, 2021), paper F2C.3.

[14] C. Caillaud, H. Bertin, A. Bobin, R. Gnanamani, N. Vaissiere, F. Pommereau, J. Decobert and C. Maneux, "Ultra Compact High responsivity Photodiodes for >100 Gbaud Applications," 2021 European Conference on Optical Communication (ECOC), Bordeaux, France, 2021, pp. 1-4, doi: 10.1109/ECOC52684.2021.9606076.

[15] Xiang, Yuluan, et al. "High-speed waveguide Ge/Si avalanche photodiode with a gain-bandwidth product of 615 GHz." Optica 9.7 (2022): 762-769.

[16] R.Gnanamani et al., "High efficiency O-Band SOA-UTC for access networks," Compound Semiconductor Week 2023 (CSW 2023), Jeju, Korea, 2023, Paper WeB3-2.

[17] T. Ishibashi, N. Shimizu, S. Kodama, H. Ito, T. Nagatsuma, and T. Furuta, "Uni-Traveling-Carrier Photodiodes" in Ultrafast Electronics and Optoelectronics, 1997, p. UC3

[18] C. Caillaud et al., "Record 2.84 THz Gain×Bandwidth of Monolithic O-Band SOA-UTC Receiver for Future Optical Networks," 2018 European Conference on Optical Communication (ECOC), Rome, Italy, 2018, pp. 1-3, doi: 10.1109/ECOC.2018.8535493.

[19] C. Caillaud, G. Glastre, F. Lelarge, R. Brenot, S. Bellini, J. –F. Paret, O. Drisse, D. Carpentier, and M. Achouche, “Monolithic integration of a semiconductor optical amplifier and a high speed photodiode with low polarization dependence loss,” IEEE Photon. Tech. Lett, vol. 24, no. 11, pp. 897–899, Jun. 1, 2012.

[20] T. Briant, P. Grangier, R. Tualle-Brouri, A. Bellemain, R. Brenot, and B. Thedrez, “Accurate determination of the noise figure of polarization-dependent optical amplifiers: theory and experiment,” J. Light. Technol., vol. 24, no. 3, pp. 1499– 1503, Mar. 2006.

[21] M. Anagnosti et al., "Record Gain x Bandwidth (6.1 THz) Monolithically Integrated SOA-UTC Photoreceiver for 100-Gbit/s Applications," in Journal of Lightwave Technology, vol. 33, no. 6, pp. 1186-1190, 15 March15, 2015, doi: 10.1109/JLT.2014.2372816.

[22] F. Pommereau *et al.*, "Realisation of semiconductor optical amplifiers with homogeneous carrier density and low noise factor," *International Conference on Indium Phosphide and Related Materials, 2005*, Glasgow, UK, 2005, pp. 102-105, doi: 10.1109/ICIPRM.2005.1517430

[23] R. Brenot et al., “Experimental study of the impact of optical confinement on saturation effects in SOA”, in proc. OFC 2005, OME50, March 2005, Anaheim, CA

[24] M. C. A. M. Koolen, “On-wafer high-frequency device characterization,” ESSDERC ’92: 22nd European Solid State Device Research conference, Sep. 1992, pp. 679–686.